J. Fluid Mech. (1980), *vol.* 101, *part* 4, *pp.* 673–686
Printed in Great Britain

Deformation of a bubble or drop in a uniform flow

By JEAN-MARC VANDEN-BROECK
AND JOSEPH B. KELLER
Departments of Mathematics and Mechanical Engineering, Stanford University

(Received 13 November 1979 and in revised form 7 March 1980)

Steady potential flow around a two-dimensional bubble with surface tension, either free or attached to a wall, is considered. The results also apply to a liquid drop. The flow and the bubble shape are determined as functions of the contact angle β and the dimensionless pressure ratio $\gamma = (p_b - p_s)/\frac{1}{2}\rho U^2$. Here p_b is the pressure in the bubble, $p_s = p_\infty + \frac{1}{2}\rho U^2$ is the stagnation pressure, p_∞ is the pressure at infinity, ρ is the fluid density and U is the velocity at infinity. The surface tension σ determines the dimensions of the bubble, which are proportional to $2\sigma/\rho U^2$. As γ tends to ∞, the bubble surface tends to a circle or circular arc, and as γ decreases the bubble elongates in the direction normal to the flow. When γ reaches a certain value $\gamma_0(\beta)$, opposite sides of the bubble touch each other. The problem is formulated as an integrodifferential equation for the bubble surface. This equation is discretized and solved numerically by Newton's method. Bubble profiles, the bubble area, the surface energy and the kinetic energy are presented for various values of β and γ. In addition a perturbation solution is given for γ large when the bubble is nearly a circular arc, and a slender-body approximation is presented for $\beta \sim \frac{1}{2}\pi$ and $\gamma \sim \gamma_0(\beta)$, when the bubble is slender.

1. Introduction

We consider the deformation of a two-dimensional gas bubble or liquid drop due to the steady potential flow of an incompressible inviscid fluid around it. We shall write 'bubble' to mean either bubble or drop. The bubble is attached to a plane wall, meeting it at the contact angle β (see figure 1). The case $\beta = \frac{1}{2}\pi$ represents half of a free bubble. The bubble is characterized by its pressure p_b and its surface tension σ, while the fluid has density ρ, pressure p_∞ at infinity and velocity U parallel to the wall at infinity. As we shall see, the shape of the bubble is determined by β and by the dimensionless parameter

$$\gamma = (p_b - p_\infty - \tfrac{1}{2}\rho U^2)/\tfrac{1}{2}\rho U^2. \tag{1.1}$$

The size of the bubble is proportional to the length $2\sigma/\rho U^2$.

We shall formulate this flow problem as a boundary-value problem in §2. Then in §3 we shall convert it into an integrodifferential equation, and in §4 present a method for solving this equation numerically. The method involves discretization, which converts the equation into a set of nonlinear algebraic equations. Then it employs Newton's method to solve these equations. This procedure can be used for any values of β and γ, and we have used it for various values of them. Some of the results obtained are shown in figures 2–8, and they are discussed in §7.

In addition to the numerical results, we present two analytical results. In §5 we

0022-1120/80/4593-2620 $02.00

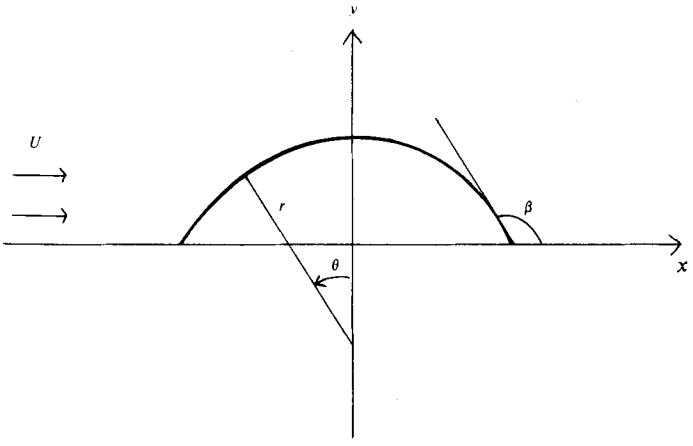

FIGURE 1. Sketch of the bubble and the co-ordinates.

give a perturbation expansion for the bubble surface valid for γ large. It shows how the surface deviates from a circular arc as γ decreases from infinity. For the free bubble ($\beta = \frac{1}{2}\pi$) the expansion is especially simple, and it agrees with the numerical results within five per cent for $\gamma > 10$. This agreement is also a check on our numerical results.

In §6 we obtain the bubble shape approximately when the bubble is slender, by using a slender-body approximation for the flow. This result is useful for $\beta \sim \frac{1}{2}\pi$ and $\gamma \sim \gamma_0(\beta)$, the value of γ at which opposite sides of the bubble just touch one another, as is shown by comparison with our numerical results. This theory can also be used for a three-dimensional bubble, as we show.

Another check on our numerical results is obtained by comparing them with the exact solution obtained by McLeod (1955) for the special case of a free bubble ($\beta = \frac{1}{2}\pi$) with $\gamma = 0$. The results agree to four significant figures.

2. Formulation as a boundary-value problem

Let us consider the steady two-dimensional potential flow of an inviscid incompressible fluid around a bubble within which the pressure has the constant value p_b (see figure 1). We assume that the bubble is symmetric about the y axis and that it makes the angle β with the x axis, which represents a rigid wall. The case $\beta = \frac{1}{2}\pi$ corresponds to the upper half of a free bubble. It is convenient to measure lengths in units of $2\sigma/\rho U^2$ and velocities in units of U. Therefore we introduce the dimensionless potential and stream functions ϕb and ψb so that their dimensional counterparts are $(2\sigma/\rho U)\,\phi b$ and $(2\sigma/\rho U)\,\psi b$. The constant $b > 0$ is to be chosen so that $\phi = \pm 1$ at the front and rear stagnation points, respectively.

We denote the streamline along the wall and along the bubble by $\psi = 0$. Then the flow region corresponds to the upper half ($\psi \geqslant 0$) of the ϕ, ψ plane. The bubble surface corresponds to the segment $|\phi| < 1$, $\psi = 0$ of the ψ axis.

We shall seek $x + iy$ as an analytic function of $\phi + i\psi$ in $\psi \geqslant 0$. At infinity we require the velocity to be U in the x direction, so the dimensionless velocity is unity in the

x direction. Therefore $x+iy$ must tend to $b(\phi+i\psi)$ at infinity. On the bubble surface the Bernoulli equation and the pressure jump due to surface tension yield

$$p_\infty+\frac{\rho U^2}{2}-\frac{\rho q^2}{2}+\sigma k=p_b, \quad |\phi|<1, \quad \psi=0. \tag{2.1}$$

Here q is the flow speed and k is the curvature of the bubble surface, counted positive when the bubble is on the concave side of the surface. In dimensionless variables this becomes

$$q^2=k-\gamma, \quad |\phi|<1, \quad \psi=0. \tag{2.2}$$

where γ is defined in (1.1).

The equation of the bubble surface is obtained from $x(\phi+i\psi)$, $y(\phi+i\psi)$ by setting $\psi=0$ and restricting ϕ to the range $|\phi|\leqslant 1$. We require that the end points of the surface be on the wall and be symmetric about the origin, and that the rest of the streamline $\psi=0$ be on the wall. These conditions yield

$$y(\phi)=0 \quad |\phi|\geqslant 1, \quad x(-1)=-x(1). \tag{2.3}$$

The condition that the contact angle be β yields

$$\lim_{\phi\to\pm 1}\frac{y_\phi(\phi)}{x_\phi(\phi)}=\pm\tan\beta. \tag{2.4}$$

In (2.4) the limit is the one-sided limit as $|\phi|$ increases. Furthermore, in (2.2) k is the curvature of the curve $x(\phi)$, $y(\phi)$. This completes the formulation of the problem of determining the constant b and the analytic function $x+iy$. This function must tend to $b(\phi+i\psi)$ at infinity in $\psi\geqslant 0$, satisfy (2.2) and (2.3) on $\psi=0$ and satisfy (2.4) at $\psi=0, \phi=\pm 1$.

3. Reformulation as an integrodifferential equation

It is convenient to reformulate the boundary-value problem as an integrodifferential equation by considering $x_\phi+iy_\phi-b$. This function is analytic in the half-plane $\psi\geqslant 0$ and vanishes at infinity. Therefore on $\psi=0$ its real part is the Hilbert transform of its imaginary part. From (2.3) we have $y_\phi=0$ on $\psi=0$, $|\phi|\geqslant 1$ and therefore the Hilbert transform yields

$$x_\phi(\phi)=b+\frac{1}{\pi}\int_{-1}^{1}\frac{y_\phi(\phi')}{\phi'-\phi}d\phi'. \tag{3.1}$$

The assumed symmetry of the bubble requires that $y(-\phi)=y(\phi)$, so we can rewrite (3.1) in the form

$$x_\phi(\phi)=b+\frac{1}{\pi}\int_0^1\left[\frac{y_\phi(\phi')}{\phi'-\phi}+\frac{y_\phi(\phi')}{\phi'+\phi}\right]d\phi'. \tag{3.2}$$

Next we express the boundary condition (2.2) in terms of x_ϕ and y_ϕ, noting that $q^2=b^2(x_\phi^2+y_\phi^2)^{-1}$. Then (2.2) becomes

$$\frac{b^2}{x_\phi^2+y_\phi^2}=\frac{y_\phi x_{\phi\phi}-x_\phi y_{\phi\phi}}{(x_\phi^2+y_\phi^2)^{\frac{3}{2}}}-\gamma, \quad |\phi|<1, \quad \psi=0. \tag{3.3}$$

Now (3.2) and (3.3) together constitute a nonlinear integrodifferential equation for $y_\phi(\phi)$ in the interval $0 \leqslant \phi \leqslant 1$. The symmetry of the bubble implies that

$$y_\phi(0) = 0. \tag{3.4}$$

The additional condition (2.4) at $\phi = 1$ completes the formulation of the problem for y_ϕ and b.

This formulation of the problem, and the numerical method used to solve it, follows closely the work of Schwartz & Vanden-Broeck (1979), Vanden-Broeck & Schwartz (1979) and Vanden-Broeck & Keller (1980).

4. Numerical procedure

To solve the problem (3.2)–(3.4) and (2.4) we find it convenient to introduce the new independent variable α in place of ϕ by the definition

$$\phi = 1 - \alpha^{\pi/\beta}. \tag{4.1}$$

This particular change of variable is chosen because near $\phi = 1$, $y_\phi(\phi)$ behaves like $(1-\phi)^{\beta/\pi-1}$, which is singular since $\beta < \pi$. The derivative $Y_\alpha(\alpha)$ of the new function $Y(\alpha) = y[\phi(\alpha)]$ is regular at $\alpha = 0$, which corresponds to $\phi = 1$. Therefore we rewrite (3.2)–(3.4) and (2.4) in terms of α, $Y(\alpha)$ and $X(\alpha) = x[\phi(\alpha)]$.

Next we introduce the N mesh points α_I defined by

$$\alpha_I = \frac{I-1}{N-1} \quad I = 1,\ldots,N. \tag{4.2}$$

We also define the N corresponding quantities

$$Y'_I = Y_\alpha(\alpha_I), \quad I = 1,\ldots,N. \tag{4.3}$$

It follows from (3.4) that $Y'_N = 0$, so only the first $N-1$ of the Y'_I are unknown. We shall also use the $N-1$ intermediate mesh points $\alpha_{I+\frac{1}{2}}$ given by

$$\alpha_{I+\frac{1}{2}} = \tfrac{1}{2}(\alpha_I + \alpha_{I+1}), \quad I = 1,\ldots,N-1. \tag{4.4}$$

We now compute $X_\alpha(\alpha_{I+\frac{1}{2}})$ in terms of the Y'_J by applying the trapezoidal rule to the integral in (3.2) rewritten in terms of the new variables, with the mesh points α_J. These points are locally symmetric about $\alpha_{I+\frac{1}{2}}$, and the quadrature formula is also symmetric. Therefore the contributions from the neighbourhood of the singularity cancel out, permitting us to evaluate the Cauchy principal value integral as if it were an ordinary integral. Then from the $X_\alpha(\alpha_{I+\frac{1}{2}})$ we compute $X_{\alpha\alpha}(\alpha_{I+\frac{1}{2}})$ and from Y'_I we compute $Y_\alpha(\alpha_{I+\frac{1}{2}})$ and $Y_{\alpha\alpha}(\alpha_{I+\frac{1}{2}})$. In all three cases we use four point difference and interpolation formulas, and obtain the results in terms of the Y'_J.

Next we substitute into (3.3), rewritten in terms of α, the expressions so obtained for X_α, $X_{\alpha\alpha}$, Y_α and $Y_{\alpha\alpha}$ at the $N-1$ points $\alpha_{I+\frac{1}{2}}$, $I = 1,\ldots,N-1$. In this way we obtain $N-1$ nonlinear algebraic equations involving the N unknowns Y'_I, $I = 1,\ldots,N-1$ and b. The Nth equation is obtained from (2.4) at $\phi = 1$, rewritten in terms of the new variables, by using a three-point Lagrange extrapolation formula to evaluate the left-hand side.

The N nonlinear equations are solved by Newton's iteration method. For each value of β and some large value of γ, the initial approximation for the bubble surface

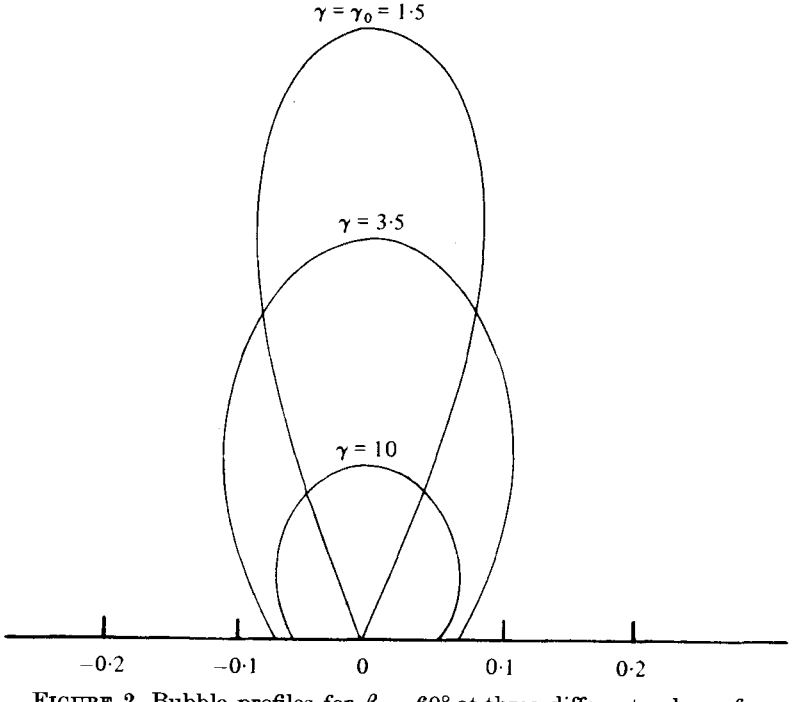

FIGURE 2. Bubble profiles for $\beta = 60°$ at three different values of γ. The vertical scale is the same as the horizontal scale. At $\gamma = \gamma_0 = 1{\cdot}5$ the bubble has just one point of contact with the wall.

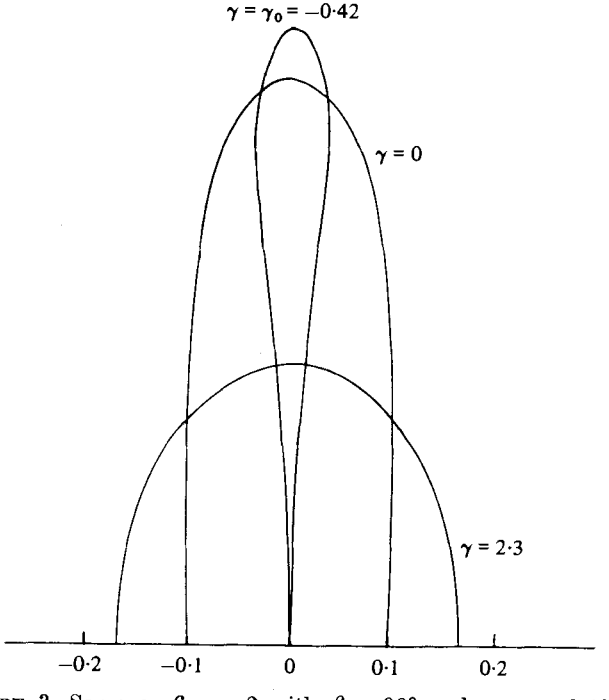

FIGURE 3. Same as figure 2 with $\beta = 90°$ and $\gamma_0 = -0{\cdot}42$. Each curve also represents half of a bubble in the absence of the wall.

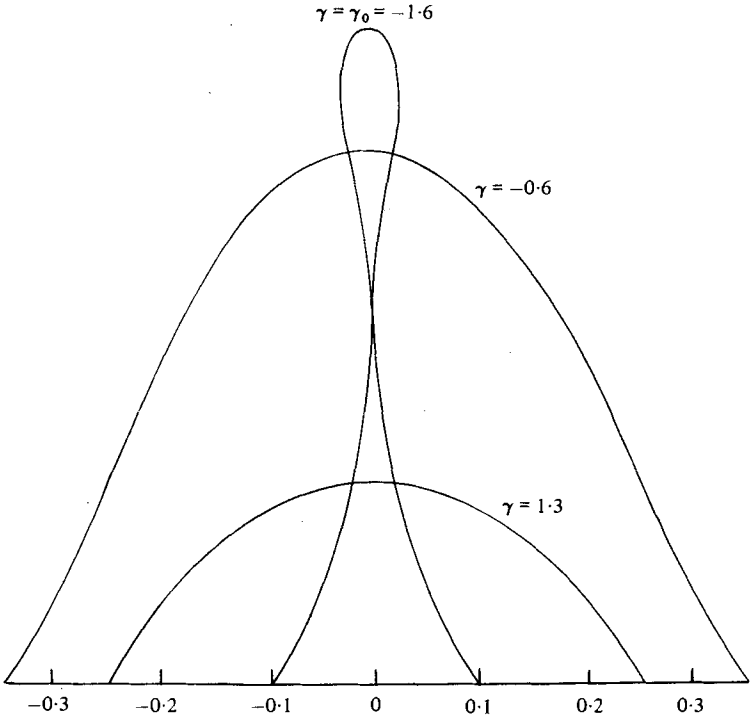

FIGURE 4. Bubble profiles for $\beta = 120°$ and three values of γ. The vertical scale is the same as the horizontal scale. At $\gamma = \gamma_0 = -1{\cdot}6$ the bubble touches itself at about the distance $y = 0{\cdot}35$ from the wall.

is taken to be the appropriate circular arc. Iterations are continued until the solution converges within the specified tolerance. This solution is then used as the initial approximation for the next smaller value of γ, and so on. After a solution for the Y_I' and b converges for given values of β and γ, the surface profile $X(\alpha)$, $Y(\alpha)$ is obtained. This is done by integrating $X_\alpha(\alpha_{I+\frac{1}{2}})$ and $Y_\alpha(\alpha_{I+\frac{1}{2}})$.

We have used this method, usually with $N = 40$, for $\beta = 45°$, $60°$, $75°$, $90°$ and $120°$. Some of the resulting bubble profiles are shown in figures 2–4, respectively. For each β, the values of γ lie in the range. $\infty > \gamma > \gamma_0(\beta)$, where $\gamma_0(\beta)$ is the value of γ at which opposite sides of the bubble touch each other at one point. For $\beta \leqslant 90°$ this point of contact is on the wall, while for $\beta > 90°$ it is off the wall. The numerical scheme can be used with $\gamma < \gamma_0(\beta)$ but it then yields a surface which crosses itself, so the fluid regions are overlapping and therefore the velocity is multiple valued. These solutions are not admissible as solutions of the physical problem. The way to obtain physically acceptable solutions for $\gamma < \gamma_0(\beta)$ is described in §7.

To test the numerical scheme, we applied it to the free bubble ($\beta = \frac{1}{2}\pi$) with $\gamma = 0$. For this case an exact analytic solution for the bubble surface was obtained by McLeod (1955). This solution gives for the ratio of the long axis of the bubble to the short axis the value 5.5. We used our numerical method in this case with $N = 30$, 40 and 50; the respective values of the axis ratio were 5·502, 5·5006 and 5·5002, in good agreement with the exact result. Furthermore the entire bubble surface obtained numerically was indistinguishable from the exact result within graphical accuracy.

Another test of the method was a comparison of the numerically computed bubble surface for the free bubble ($\beta = \frac{1}{2}\pi$) with the perturbation result of §5. For $\gamma > 10$ the two results for the bubble radius as a function of angle differed by less than five per cent.

From the numerical solution we can calculate not only the shape of the bubble surface but also the kinetic and potential energies T and V. The potential energy V is the energy of the bubble surface, which is equal to the surface tension σ times the length of the surface. In dimensional variables

$$V = (2\sigma^2/\rho U^2)\int_{-1}^{1} [x_\phi^2(\phi) + y_\phi^2(\phi)]^{\frac{1}{2}}\, d\phi. \tag{4.5}$$

The kinetic energy T is the kinetic energy of the fluid in a frame of reference in which the fluid at infinity is at rest. Thus it is the kinetic energy of the fluid when the bubble is moving through it, and is given by

$$T = (2\sigma^2/\rho U^2)\iint [(u-1)^2 + v^2]\, dx\, dy. \tag{4.6}$$

Here u and v are the dimensionless x and y components of velocity of the fluid, and the integration extends over the fluid region.

The integral over the fluid region in (4.6) can be converted into an integral over the bubble surface by first restricting the integration to the domain D_{ad} outside the bubble and inside the rectangle $-a < x < a$, $0 < y < d$. Later we shall let a and d tend to infinity. Thus we can write T as follows, and then rewrite it using the facts that $u^2+v^2 = b^2\partial(\phi,\psi)/\partial(x,y)$ and that $u = x_\phi b^{-1}(u^2+v^2)$:

$$\left.\begin{aligned} T(2\sigma^2/\rho U^2)^{-1} &= \lim_{a,\,d\to\infty} \int_{D_{ad}} \int [(u^2+v^2) - 2u + 1]\, dx\, dy \\ &= \lim_{a,\,d\to\infty} \int_{D_{ad}} \int [b^2 d\phi\, d\psi - 2b x_\phi\, d\phi\, d\psi + dx\, dy]. \end{aligned}\right\} \tag{4.7}$$

In the second line of (4.7) the integral of $dx\,dy$ is just $2ad - A$ where A is the area of the bubble and $2ad$ is the area of the rectangle. The integral of $b^2 d\phi\, d\psi$ is b^2 times the area of the image of D_{ad} in the ϕ, ψ plane, which tends to the area of the rectangle as a and d tend to infinity.

By using these facts in (4.7) and using the Cauchy–Riemann relation $x_\phi = y_\psi$, we can write T in the form

$$T(2\sigma^2/\rho U^2)^{-1} = \lim_{a,\,d\to\infty} [4ad - A - 2b\int_{D_{ad}} \int y_\psi\, d\psi\, d\phi]. \tag{4.8}$$

The integral over ψ yields y at the upper limit, which is d, minus y at the lower limit, which is zero except on the bubble. Then the integral of d with respect to ϕ yields $-4ad$. Thus (4.8) becomes

$$\left.\begin{aligned} T &= (2\sigma^2/\rho U^2)\left[2b\int_{-1}^{1} y(\phi)\, d\phi - A\right] \\ &= (2\sigma^2/\rho U^2)\int_{-1}^{1} y(\phi)[2b - x_\phi(\phi)]\, d\phi. \end{aligned}\right\} \tag{4.9}$$

In the last line we have used the dimensionless integral for A which occurs in the formula

$$A = (2\sigma/\rho U^2)^2 \int_{-1}^{1} y(\phi)\, x_\phi(\phi)\, d\phi. \tag{4.10}$$

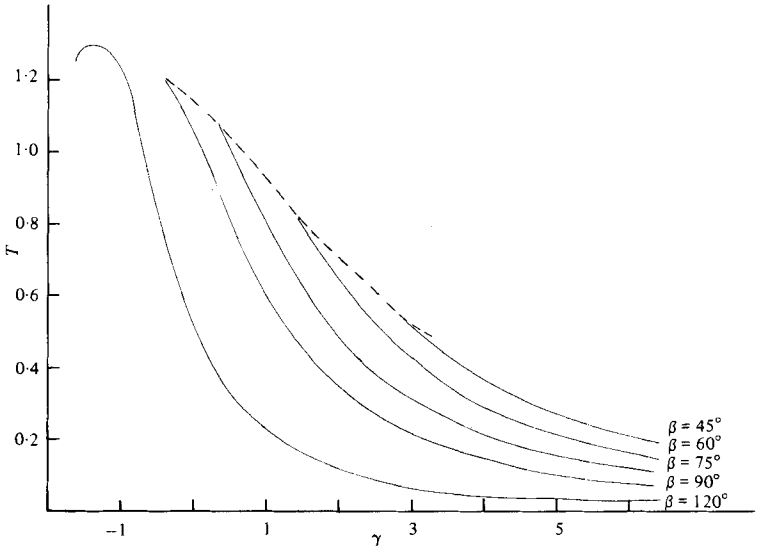

FIGURE 5. Values of the kinetic energy T in units of $2\sigma^2/\rho U^2$ as a function of γ for five values of β. The dashed curve corresponds to the family of bubbles having one point of contact with the wall.

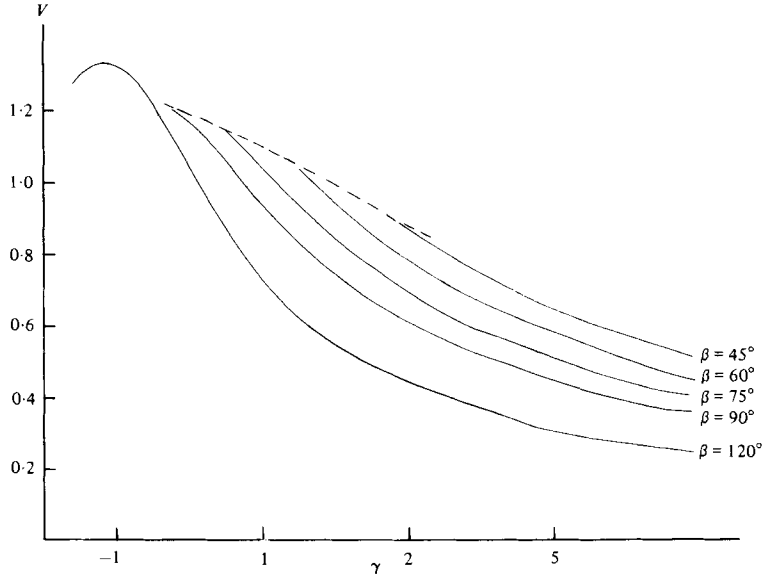

FIGURE 6. Values of the potential energy V in units of $2\sigma^2/\rho U^2$ as a function of γ for five values of β. The dashed curve corresponds to the family of bubbles having one point of contact with the wall.

The integrals in (4.5), (4.9) and (4.10) can be evaluated by the trapezoidal rule, using the previously obtained values of the quantities in the integrands. We have evaluated them for different values of β. For each β the results for T, V and A are shown as functions of γ in figures 5, 6 and 7 respectively. The dashed curve corresponds to the family of bubbles with one point of contact on the wall, discussed in §7.

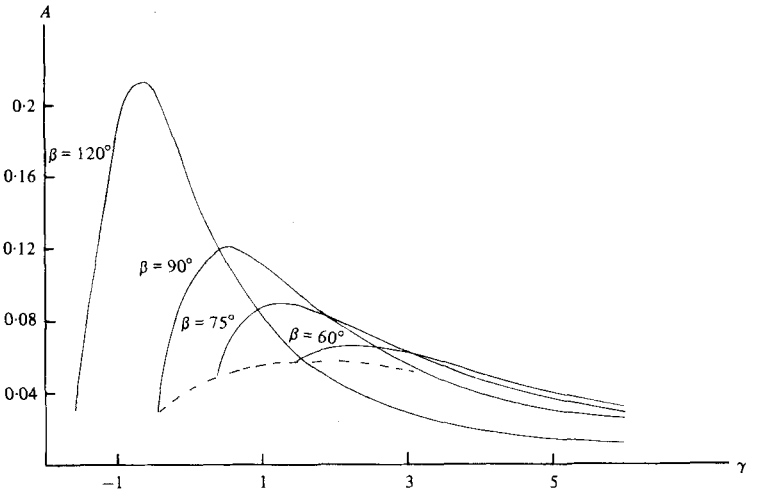

FIGURE 7. Values of the bubble area A in units of $(2\sigma/\rho U^2)^2$ as a function of γ for four values of β. The dashed curve corresponds to the family of bubbles having one point of contact with the wall. The ordinate is also equal to the square of the Weber number W, defined by $W^2 = A(\rho U^2/2\sigma)^2$.

5. Perturbation expansion for γ large

As $\gamma \to \infty$ we conclude from (2.2) that $k \sim \gamma$, so the bubble surface tends to a circular arc of dimensionless radius γ^{-1}. The angular width of this arc is $2(\pi - \beta)$ since it must make the angle β with the x axis at each of its endpoints. We wish to use this result as the first term in a perturbation expansion of the bubble surface in powers of γ^{-1}. To this end we introduce polar co-ordinates r, θ with origin on the y axis at $y = -\gamma^{-1}$ and with θ measured counterclockwise from this axis. To simplify the analysis we assume that the bubble is symmetric about this axis (see figure 1). Then we seek the bubble surface in the form $r = r(\theta, \gamma)$ with θ in the range $|\theta| \leqslant \hat{\theta}(\gamma)$. The leading terms in $r(\theta, \gamma)$ and $\hat{\theta}(\gamma)$ are given by the circular arc result so we write

$$r(\theta, \gamma) = \gamma^{-1} + \gamma^{-2} r_1(\theta) + \dots, \tag{5.1}$$

$$\hat{\theta}(\gamma) = \pi - \beta + \gamma^{-1}\theta_1 + \dots. \tag{5.2}$$

We also write the flow speed $q(\theta, \gamma)$ in the form

$$q(\theta, \gamma) = q_0(\theta) + \dots. \tag{5.3}$$

To determine $r_1(\theta)$ and θ_1 we shall use (2.2), (2.4), the condition that the end points of the bubble surface lie on the x axis, and the symmetry condition $r'(0, \gamma) = 0$. These conditions are

$$q^2 = (r^2 + 2r'^2 - rr'')(r^2 + r'^2)^{-\frac{3}{2}} - \gamma, \tag{5.4}$$

$$\beta = \frac{\pi}{2} - \hat{\theta}(\gamma) + \tan^{-1}\frac{r[\hat{\theta}(\gamma), \gamma]}{r'[\hat{\theta}(\gamma), \gamma]}, \tag{5.5}$$

$$r[\hat{\theta}(\gamma), \gamma] \cos\hat{\theta}(\gamma) = \gamma^{-1} \cos(\pi - \beta), \tag{5.6}$$

$$r'(0, \gamma) = 0. \tag{5.7}$$

We now substitute (5.1)–(5.3) into (5.4)–(5.7) and obtain from the coefficients of the leading power of γ in each equation the results

$$r_1''(\theta)+r_1(\theta) = -q_0^2(\theta), \tag{5.8}$$

$$\theta_1 = -r_1'(\pi-\beta), \tag{5.9}$$

$$r_1(\pi-\beta)\cos(\pi-\beta) = \theta_1 \sin(\pi-\beta), \tag{5.10}$$

$$r_1'(0) = 0. \tag{5.11}$$

Upon eliminating θ_1 and solving the resulting equations for $r_1(\theta)$ we obtain

$$r_1(\theta) = -\int_0^{\theta} q_0^2(z)\sin(\theta-z)\,dz - \sec 2\beta \int_0^{\pi-\beta} q_0^2(z)\sin(z+2\beta)\,dz\cos\theta. \tag{5.12}$$

Then θ_1 is given by using this result in (5.9) or (5.10).

The function $q_0(\theta)$ in (5.12) is the speed of the flow past a circular arc attached to a plane. It is given by $q_0(\theta) = \gamma|\partial_\theta \phi_0(\gamma^{-1},\theta)|$ in terms of the potential $\phi_0(r,\theta)$. By using the Kármán–Trefftz transformation we find

$$\phi_0(\gamma^{-1},\theta) = \frac{\pi\sin\beta}{\beta\gamma}\frac{[1-\cos(\theta+\beta)]^{\pi/\beta}-[\cos\theta-\cos\beta]^{\pi/\beta}}{[1-\cos(\theta+\beta)]^{\pi/\beta}+[\cos\theta-\cos\beta]^{\pi/\beta}}. \tag{5.13}$$

In the special case of a free bubble ($\beta = \frac{1}{2}\pi$) we find by using (5.13) that $q_0(\theta) = 2|\cos\theta|$ and then (5.12) yields $r_1(\theta) = -\frac{4}{3}(1+\sin^2\theta)$. Now (5.9) gives $\theta_1 = 0$, which is to be expected since in this case $\hat{\theta}(\gamma) = \frac{1}{2}\pi$ by symmetry. Finally (5.1) becomes

$$r(\theta,\gamma) = \gamma^{-1}-\tfrac{4}{3}\gamma^{-2}(1+\sin^2\theta)+\ldots. \tag{5.14}$$

Thus to this order the bubble is an ellipse with its short axis along the flow direction.

The preceding results can be used to evaluate for γ large, the quantities V, T and A given by (4.5), (4.9) and (4.10). The first term in (5.1) for $r(\theta,\gamma)$ yields

$$V = (2\sigma^2/\rho U^2)\,2(\pi-\beta)\gamma^{-1}+O(\gamma^{-2}), \tag{5.15}$$

$$A = (2\sigma/\rho U^2)^2(\pi-\beta+\tfrac{1}{2}\sin 2\beta)\gamma^{-2}+O(\gamma^{-3}). \tag{5.16}$$

The corresponding result for T can be found similarly.

6. Slender-body approximation

The numerical results presented in the preceding sections show that the bubble is very slender for $\beta \sim \frac{1}{2}\pi$ and $\gamma \sim \gamma_0(\beta)$. This is evident in figure 3 and even in figure 4. Therefore we shall use slender-body theory to get an approximate description of the flow around the bubble. Then we shall use this flow in the boundary condition (2.2) to obtain a differential equation for the bubble surface. By solving this equation subject to suitable boundary conditions, we shall obtain an approximation to the bubble surface.

The flow about a slender body can be represented by both uniform and non-uniform asymptotic expansions in the slenderness ratio of the body. We shall use only the leading term in the non-uniform expansion, which is the flow about a flat plate lying along the center line of the body. We denote the half-width of the plate by a, which is to be found. Then the plate and its image lie on the y axis with the ends at $y = \pm a$.

We need the dimensionless potential function $b\phi(x, y)$ for flow about this plate, which represents a uniform flow in the x direction at infinity. It is readily found, and on the plate it is given by

$$b\phi(0, y) = (a^2 - y^2)^{\frac{1}{2}}, \quad -a \leqslant y \leqslant a. \tag{6.1}$$

From (6.1) we find for the speed of the flow along the plate

$$q^2(0, y) = y^2(a^2 - y^2)^{-1}. \tag{6.2}$$

The variables are non-dimensionalized as in § 2.

Let us write the equation of the bubble as $x = \pm\eta(y)$, $0 \leqslant y \leqslant a$. Then the contact-angle condition (2.4) becomes

$$\eta_y(0) = -\tan(\beta - \tfrac{1}{2}\pi). \tag{6.3}$$

In addition the two sides of the bubble must meet at $y = a$, so we have

$$\eta(a) = 0. \tag{6.4}$$

Now we use (6.2) for q^2 in the boundary condition (2.2), and also approximate the curvature k by $-\eta_{yy}$. Then (2.2) becomes

$$\eta_{yy} = -y^2(a^2 - y^2)^{-1} - \gamma, \quad 0 \leqslant y \leqslant a. \tag{6.5}$$

Upon integrating (6.5) twice and using (6.3) and (6.4) we obtain

$$\begin{aligned}\eta(y) = {} & (a^2 - y^2)(\gamma - 1)/2 - \tfrac{1}{2}a(a+y)\log(a+y) \\ & - \tfrac{1}{2}a(a-y)\log(a-y) + a^2\log 2a + + (a-y)\tan(\beta - \tfrac{1}{2}\pi).\end{aligned} \tag{6.6}$$

To determine the constant a, we shall use the condition that the downward force due to surface tension must be balanced by the upward force due to the negative pressure at the end of the bubble $y = a$. The surface tension exerts the downward force 2σ while the flow exerts the upward suction force $\pi\rho A^2/4$ (see Batchelor 1967, p. 412, equation (6.5.4)). Here A is the coefficient which occurs when $b\phi$ is written as $b\phi \sim Ar^{\frac{1}{2}}\cos\frac{1}{2}\theta$ in terms of polar co-ordinates with origin at the end of the plate. Upon equating these two forces we obtain

$$2\sigma = \pi\rho A^2/4. \tag{6.7}$$

In terms of the dimensionless variables introduced in § 2, this becomes

$$A^2 = 4/\pi. \tag{6.8}$$

For the potential function $b\phi$ given by (6.1) we see that $A = (2a)^{\frac{1}{2}}$, so (6.8) yields

$$a = 2/\pi. \tag{6.9}$$

The result (6.6) for $\eta(y)$ with $a = 2/\pi$ is found to give a fair approximation to the bubble surface for $\beta \sim \frac{1}{2}\pi$ and $\gamma \sim \gamma_0(\beta)$, when the bubble is slender. To illustrate this, we shall use (6.6) to calculate $\gamma_0(\frac{1}{2}\pi)$. We set $\beta = \frac{1}{2}\pi$ and $\eta(0) = 0$ in (6.6) and solve for γ, obtaining

$$\gamma_0(\tfrac{1}{2}\pi) = 1 - 2\log 2 \approx = -0{\cdot}39. \tag{6.10}$$

This is in fair agreement with the result $\gamma_0(\frac{1}{2}\pi) = -0{\cdot}42$ which we found numerically.

A similar theory can be developed for the flow past a three-dimensional bubble without a wall. Then the flow is axisymmetric about the direction of the flow at

infinity, which we take to be the x axis. When the bubble is 'slender' the flow about it is approximately that past a flat circular disk of radius a, which is to be found. By proceeding as above we obtain for the profile curve of the bubble $\eta(y)$, and for a, the dimensionless results

$$\eta(y) = -\frac{y^2}{\pi^2}+\frac{\gamma}{4}y^2+\frac{a^2}{\pi^2}\int_1^{1-y^2/a^2}\frac{\ln x}{1-x}\,dx+\frac{a^2}{\pi^2}-\frac{\gamma a^2}{4}-\frac{a^2}{6}, \tag{6.11}$$

$$a = \tfrac{1}{2}\pi. \tag{6.12}$$

From (6.11), to find when opposite sides of the bubble just touch at $y = 0$, we set $\eta(0) = 0$. This yields for γ the critical value

$$\gamma_0 = 4\pi^{-2}-\tfrac{2}{3} = -0{\cdot}26. \tag{6.13}$$

We shall compare these results with numerical calculations when the calculations are completed.

7. Discussion of results

It is helpful to introduce the Weber number $W = A^{\frac{1}{2}}(\rho U^2/2\sigma)$ which can be found from (4.10). In figure 7 the ordinate is W^2, so we see that for each value of β there is a maximum value of the Weber number above which there is no steady solution of the kind considered here. When $\beta = 90°$ the maximum value is $W^2 \sim 0{\cdot}12$, and it occurs at $\gamma \sim 0{\cdot}8$. On the solution branch to the right of the maximum in figure 7, W^2 decreases as γ increases, while from figure 6, V also decreases as γ increases. Thus on this right branch V decreases as W decreases, so the solution is probably stable. In a similar way we see that the branch to the left of the maximum is probably unstable.

The asymptotic analysis of §5 shows that as γ tends to infinity, the bubble surface tends to an arc of a circle of radius $2\sigma/\rho U^2\gamma$. As γ decreases from infinity, the bubble elongates in the direction normal to the flow. For $\beta = \frac{1}{2}\pi$, which corresponds to a free bubble, the surface becomes elliptical with the axis ratio $1+\frac{4}{3}\gamma+O(\gamma^{-2})$, the long axis being normal to the flow direction. To describe the subsequent distortion of the bubble, it is convenient to consider separately the cases $\beta \leqslant \frac{1}{2}\pi$ and $\beta \geqslant \frac{1}{2}\pi$.

For $\beta \leqslant \frac{1}{2}\pi$ the two points where the bubble surface touches the wall at first move apart as γ decreases. They reach a maximum separation, then get closer together, and finally meet when γ reaches the critical value $\gamma_0(\beta)$. This behaviour can be seen in the bubble profiles shown in figures 2–4, and it is displayed explicitly in figure 8.

For $\beta \geqslant \frac{1}{2}\pi$ the behaviour is initially similar, but γ can be decreased to zero without opposite sides of the bubble touching. At $\gamma = 0$ the curvature of the bubble surface becomes zero at the two points where it touches the wall. This is because they are stagnation points, at which the pressure in the fluid is the stagnation pressure $p_s = p_\infty + \frac{1}{2}\rho U^2$. The condition $\gamma = 0$ means that the bubble pressure p_b equals p_s, so the curvature of the surface is zero at these points. When γ is decreased further, to negative values, opposite sides of the bubble come closer together until they touch at a negative critical value $\gamma_0(\beta) < 0$. The contact points are away from the wall for $\beta > \frac{1}{2}\pi$, and at the wall for $\beta = \frac{1}{2}\pi$, the free bubble case.

To obtain physically acceptable solutions for $\gamma < \gamma_0(\beta)$ we consider first the case $\beta < \frac{1}{2}\pi$. We assume that in this case the bubble surface will have just one point of contact with the wall, at which the two ends of the bubble surface meet. If we adjoin

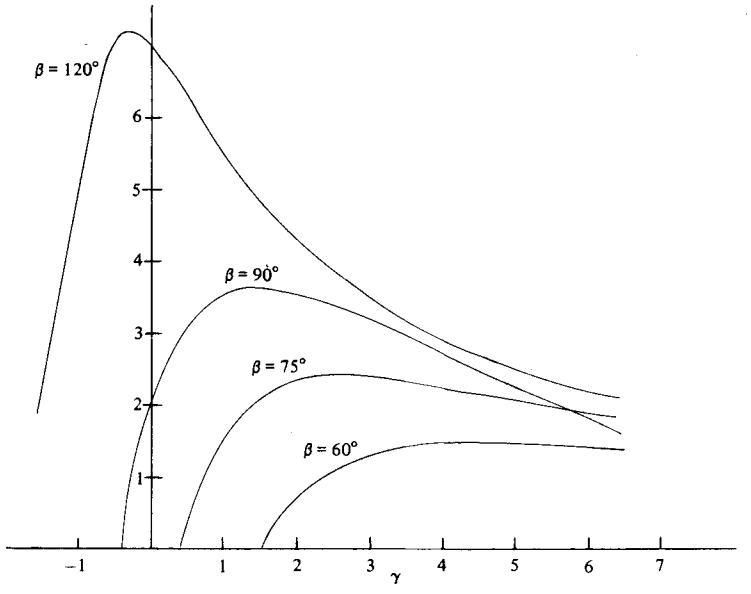

FIGURE 8. Values of the distance Δx between the stagnation points as a function of γ for four values of β.

this extra condition to the previously formulated problem, we cannot expect to find a solution when $\gamma < \gamma_0(\beta)$. This is because we have added one extra condition and no extra unknowns. This difficulty can be overcome by not specifying the value of β, but considering it to be an unknown. This makes sense physically because of the invalidity of the usual argument which determines β to make the interfacial forces balance at the contact point. When two surfaces meet there symmetrically, the symmetry guarantees a force balance for any β.

The problem just posed has already been solved by our previous computations. For each $\beta \leqslant \frac{1}{2}\pi$ we have found a solution with just one point of contact with the wall when $\gamma = \gamma_0(\beta)$. If γ is specified then there is a solution of this kind with β given by the inverse function

$$\beta = \gamma_0^{-1}(\gamma), \quad \gamma \geqslant \gamma_0(\tfrac{1}{2}\pi). \tag{7.1}$$

As γ tends to infinity, it follows from (7.1) that β tends to zero. Then the bubble tends to a circle of radius $2\sigma/\rho U^2\gamma$ tangent to the wall. In figures 5–7 the values of T, V and A for this family of bubbles are shown by dashed curves.

We could have obtained solutions for $\beta \geqslant \frac{1}{2}\pi$ and $\gamma < \gamma_0(\beta)$ by using the technique presented by Vanden-Broeck & Keller (1980). However we did not do so because the pinched bubble consisting of two sub-bubbles is probably unstable. It is likely that the two sub-bubbles will separate from one another.

Finally let us mention the relation of our results to the problem of flow past a bubble which is at a distance d from a wall. The two parameters d and γ characterize such a flow and the resulting bubble. For $d \to \infty$, the bubble tends to the free bubble corresponding to our present results with $\beta = \frac{1}{2}\pi$. As d decreases for a fixed value of γ, the two stagnation points on the bubble must move toward the end of the bubble nearest the wall. They coalesce at the contact point when the bubble just touches the wall. Then the contact angle β is given as a function of γ by (7.1) while the bubble shape and

the flow are given by our solution corresponding to (7.1). Thus the two extreme cases $d = \infty$ and $d = 0$ of this family of bubbles are given by the present calculations.

We wish to thank Prof. Lu Ting for some very helpful discussions of this problem and Prof. Paul Garabedian for bringing to our attention the work of his former student McLeod. This work was supported by the Office of Naval Research, the Army Research Office, the Air Force Office of Scientific Research and the National Science Foundation.

REFERENCES

BATCHELOR, G. K. 1967 *Introduction to Fluid Dynamics*. Cambridge University Press.

MCLEOD, E. B. 1955 *J. Rat. Mech. Anal.* **4**, 557.

SCHWARTZ, L. W. & VANDEN-BROECK, J.-M. 1979 *J. Fluid Mech.* **95**, 119.

VANDEN-BROECK, J.-M. & KELLER, J. B. 1980 *J. Fluid Mech.* **98**, 161.

VANDEN-BROECK, J.-M. & SCHWARTZ, L. W. 1979 *Phys. Fluids* **22**, 1868.